

Resonant Raman Scattering in $\text{YBa}_2\text{Cu}_3\text{O}_7$: Band Theory and Experiment

E. T. Heyen, S. N. Rashkeev,^(a) I. I. Mazin,^(a) O. K. Andersen, R. Liu, M. Cardona, and O. Jepsen

*Max-Planck-Institut für Festkörperforschung, Heisenbergstrasse 1, D-7000 Stuttgart 80,
Federal Republic of Germany*

(Received 14 August 1990)

We have measured and calculated the dependence of the Raman phonon intensities of $\text{YBa}_2\text{Cu}_3\text{O}_7$ on laser frequency. The local-density approximation and the linear muffin-tin-orbital method were used for the calculations. We find good agreement not only in the absolute phonon intensities in zz or xx/yy polarization but also in the shape of the resonance profiles. These results indicate that the local-density approximation gives an essentially correct description of the band structure and of the electron-phonon interaction ± 2 eV around the Fermi energy. We interpret our data in terms of specific interband transitions and estimate the mode mixing.

PACS numbers: 74.70.Vy, 71.10.+x, 78.20.-e, 78.30.Er

Raman scattering has been used intensively to study high-temperature superconductors.¹ It is possible not only to investigate the vibrational properties, but also to estimate electron-phonon coupling constants,² and to measure the superconducting gap in electronic Raman scattering.¹ From the dependence of the absolute efficiency for phonon scattering on laser energy [resonant Raman scattering (RRS)] one may, with the help of a suitable theoretical model, obtain information about the electronic structure. Preliminary RRS results have been published with the scattering efficiency in arbitrary units,^{3,4} but no theoretical analysis was attempted so far. Here, we present experimental and band-theoretical absolute RRS profiles for $\text{YBa}_2\text{Cu}_3\text{O}_7$.

The Raman efficiency for scattering by an optical phonon at low temperature is given by

$$S_{is}(\omega) = \frac{V}{(4\pi)^2} \left(\frac{\omega}{c} \right)^4 \left| \frac{d\epsilon_{is}(\omega)}{dQ} \right|^2. \quad (1)$$

i and s are the polarization directions of the incident and scattered light, ω is the laser frequency, V is the unit-cell volume, c is the light velocity, ϵ_{is} is the complex dielectric tensor, and Q is the phonon normal coordinate. The displacement of the n th atom is $Q\mathbf{e}_n(\hbar/2M_n\omega_{\text{ph}})^{1/2}$, where \mathbf{e}_n and ω_{ph} are the phonon eigenvector and frequency.

We have measured Raman spectra of a superconducting crystal of $\text{YBa}_2\text{Cu}_3\text{O}_7$ ($T_c = 90$ K) at 10 K with thirteen energies between 1.8 and 2.7 eV of Ar^+ and Kr^+ lasers for light polarized in the xx/yy as well as in the zz directions. Since the crystal was twinned, we cannot distinguish x and y . We consider only the five A_g -symmetry phonons with energies of 500, 435, 340, 150, and 115 cm^{-1} corresponding, respectively, to motions in the z direction of O(4) (apical oxygen), O(3)+O(2) (plane oxygen in phase), O(3)-O(2) (out of phase), Cu(2) (plane copper), and Ba.⁵ Calculations suggest that the oxygen modes,⁶⁻⁸ as well as the Cu(2) and Ba modes,^{6,7} are mixed. The Raman intensities were obtained by fitting the data with Lorentz or Fano line shapes. After accounting for absorption, reflection, and

refraction by using ellipsometric data,⁹ we obtained the absolute Raman efficiency by comparing it with that of¹⁰ BaF_2 (see Fig. 1).

In spite of doubts cast on the relevance of the local-density approximation (LDA) band theory for high-

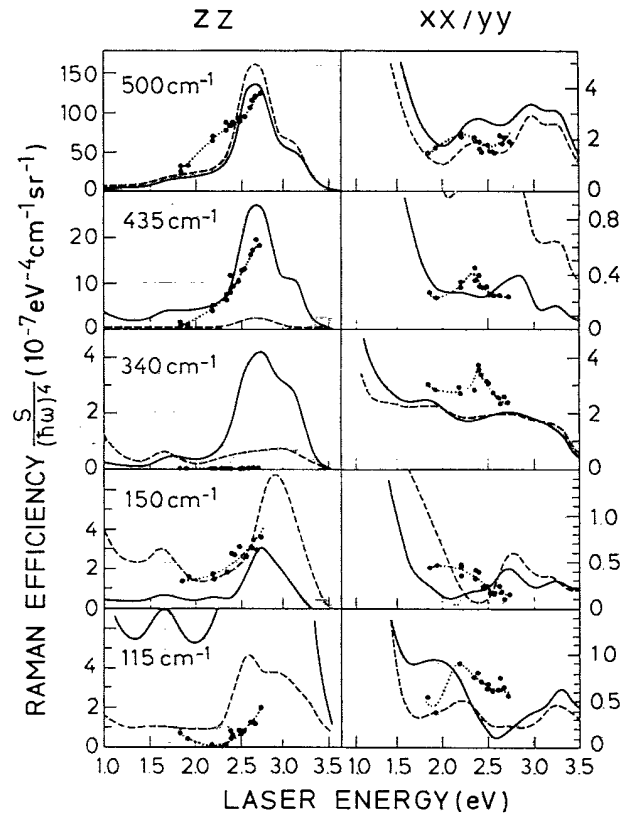


FIG. 1. Measured (large dots, the dotted line is just a guide to the eye) and calculated Raman efficiency $S/(\hbar\omega)^4$ for the five A_g phonons at 115, 150, 340, 435, and 500 cm^{-1} in zz (left-hand column) and xx/yy polarizations (right-hand column, xx and yy polarizations averaged since the crystal is twinned). For the calculations, we used either a mode mixing according to Ref. 6 (solid lines) or the pure modes (dashed lines).

temperature superconductors, it is so far the only *ab initio* theory which has yielded quantitatively correct optical^{9,11} and x-ray-absorption¹² spectra. Even for insulating $\text{YBa}_2\text{Cu}_3\text{O}_6$, the LDA gives reasonable optical spectra for energies above the gap.¹³ Moreover, the LDA was recently used successfully to calculate the frequencies and eigenvectors of optical phonons as well as the electron-phonon interaction in $\text{YBa}_2\text{Cu}_3\text{O}_7$.^{6,7} This motivated us to use it for evaluating the RRS spectra.

The self-consistent energy-band calculations for the undistorted and the five phonon-distorted structures were performed with the linear muffin-tin-orbital (LMTO) method in the atomic-spheres approximation including the combined correction.¹⁴ For the evaluation of optical matrix elements, the latter was omitted.¹¹ The interband energies are 0.0–0.4 eV higher than those obtained from the more accurate full-potential LMTO method used in the phonon calculation.⁶ The atomic sphere radii were 1.9, 2.1, 1.3, 1.1, and 0.8 Å for the Y, Ba, Cu, O, and empty spheres, respectively. All partial waves with $l \leq 3$ were included in the Y, Ba, and Cu spheres, those with $l \leq 2$ in the O spheres, and those with $l \leq 1$ in the empty spheres. The imaginary parts of the interband dielectric functions, $\epsilon_2(\omega)$, were calculated using tetrahedron integration over 147 nonequivalent \mathbf{k} points (for details, see Refs. 14 and 15 of Ref. 11). A Lorentzian broadening with a half-width of 0.12 eV, which was found to reproduce best the RRS and $\epsilon_2(\omega)$ data,⁹ was applied for all energies, modes, and polarizations to simulate lifetime effects. Figure 2 shows the broadened ϵ_2 for zero displacement. The real parts $\epsilon_1(\omega)$ were obtained by Kramers-Kronig transformation. The ϵ 's were differentiated numerically with respect to the atomic displacements and the derivatives were computed using the pure modes as well as the theoretical eigenvectors⁶ for the mixed modes. The results are shown in Fig. 1 (pure modes as dashed lines, mixed modes as solid lines). The contribution from the intraband ϵ was negligible for the

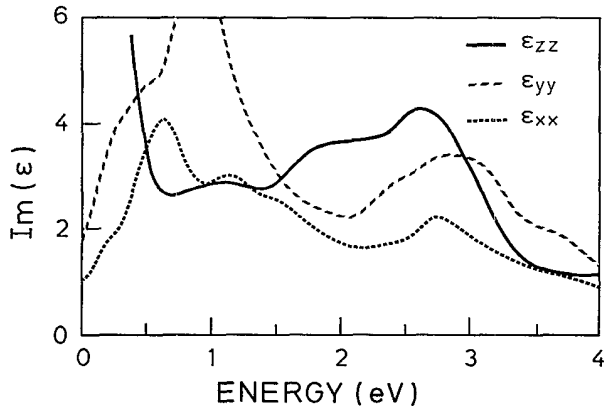


FIG. 2. Calculated imaginary part ϵ_2 of the dielectric function in z (solid line), y (dashed line), and x (dotted line) polarizations (lifetime broadening of 0.12 eV).

laser frequencies of interest.

Next we describe the experimental RRS spectra in Fig. 1, compare them with the calculation, and give an interpretation. Those spectra show the following: (a) For zz polarization, the 500- cm^{-1} mode (we omit " cm^{-1} " below) is an order of magnitude stronger than the 435 mode and 2 orders stronger than the rest. (b) The 500, 435, and 150 modes are at least an order of magnitude stronger for zz than for xx/yy . The 115 mode has similar activity for both polarizations, and the 340 mode is not observed for zz , but is the strongest mode for xx/yy . (c) At $\hbar\omega = 2.4$ eV it is known¹⁵ that the 500, 150, and 115 modes are stronger for yy than for xx , while the 340 mode is stronger for xx . (d) Some modes exhibit characteristic resonant behavior: For zz the 500, 435, and 150 modes increase strongly over the measured energy range while the 115 mode increases from a deep, flat minimum around 2.2 eV. For xx/yy the 500 mode has weak maxima and minima around 2.2 and 2.5 eV, the 435 and 340 modes have sharp maxima at 2.3 and 2.4 eV, respectively, the 150 modes seems to decrease from a flat maximum at 2.1 eV, and the 115 mode has a maximum at 2.2 eV.

The agreement between theory and experiment is remarkable considering the fact that the only adjustable parameter in the theory was the global broadening (0.12 eV): The features (a) and (b) are correctly reproduced for intensities varying by 3 orders of magnitude. For the 115 mode, however, this applies only if the mixing with the pure Cu(2) mode is substantially less than that predicted in Refs. 6 and 7, and also the small mixing of O(4) character into the 340 mode seems to be overestimated. The xx - yy anisotropy (c) of the oxygen modes (not shown in Fig. 1) is correctly reproduced, whereas no significant anisotropy is calculated for the Ba and Cu(2) modes. For the dependence on laser energy (d) the agreement is reasonable (and would have been better with the full-potential method, as judged from the bands). This warrants an interpretation in terms of the LDA bands.

Within the 3-eV range of interest there are only three possible *final*-state bands¹⁶ above E_F : the antibonding O(4)(z)-Cu(1)($z^2 - y^2$)-O(1)(y) chain band (which we shall simply refer to as "the chain band") and the two nearly degenerate antibonding O(2)(x)-Cu(2)($x^2 - y^2$)-O(3)(y) plane bands (which we call "the plane bands"). The dispersion of the chain band is, crudely speaking, $4.8[1 + \sin^2(\frac{1}{2}bk_y)]^{1/2} - 5.1$ eV, relative to E_F , while that of a plane band is $4.8[\sin^2(\frac{1}{2}ak_x) + \sin^2(\frac{1}{2} \times bk_y)]^{1/2} - 5.1$ eV. Below E_F there are many, less dispersive, Cu 3d and 2p bands.

We first interpret the calculated results for zz polarization. Above 0.5 eV, $\epsilon_{zz}(\omega)$ (Fig. 2) forms a 3-eV-wide structure which is partly due to transitions to the chain band from antibonding O(2)(z)-O(3)(z)-Cu(2)-(3 $z^2 - 1$)-O(4)(z)-O(1)(z) bands. [The Cu(2)(3 z^2

-1) orbital and the plane-oxygen z orbitals couple because the planes dimple.] These transitions have charge-transfer character with matrix elements $\langle i|z|f\rangle$ contributed by $\langle 3z^2-1|z|z\rangle$ on Cu(2), $\langle z|z|s\rangle$ on O(4), $\langle z|z|s\rangle$ on O(1), and $\langle z|z|z^2-y^2\rangle$ on Cu(1). The Cu(2)(z) and Cu(1)(z) characters originate from the tail of the O(4)(z) orbital, and the O(4)(s) and O(1)(s) characters from the tail of the Cu(1)(z^2-y^2) orbital. The ϵ_2 structure is well described as the sum of three step-ups at $\hbar\omega = 0.65, 1.65,$ and 2.50 eV, plus two step-downs at 2.90 and 3.15 eV. The step-ups at 0.65 and 1.65 eV mark the onset of transitions to the chain-band Fermi surface, the step-up at 2.50 eV the onset (near the S point) of transitions to the flattop of the chain band around the $k_y = \pi/b$ plane, and the step-down at 2.90 and 3.15 eV the end of those transitions. The initial-state band is nearly flat, as is the top of the chain band, and the matrix elements are large.

If now the position Ω (and/or the width Γ) of an ϵ_2 step is modulated by a phonon, the RRS profile develops a Lorentzian peak because, for a step of height πH (> 0 for step-down, < 0 for step-up), $\epsilon(\omega) = H \ln(\omega - \Omega + i\Gamma)$, so that

$$|\epsilon'(\omega)|^2 = H^2[(\Omega')^2 + (\Gamma')^2][(\omega - \Omega)^2 + \Gamma^2]^{-1}$$

(the prime denotes d/du , u equals the displacement of all equivalent atoms, away from the chains). If H is also modulated, additional less resonant terms occur. The chain band is particularly sensitive to O(4) displacements along the z direction because they modulate the short O(4)-Cu(1) and O(4)-O(1) distances and thereby the large hopping integrals. Because of the importance of O(4)-O(1) hopping, the deformation potential is largest at the top of the chain band ($\hbar\Omega' \approx -4.5$ eV/Å). The top of the initial-state O(2)(z)-Cu(2)($3z^2-1$)-O(4)(z) band responds to O(4) displacements in the opposite direction, but weaker (≈ 1.5 eV/Å), because the Cu(2)-O(4) distance is considerably larger. These transitions to the top of the chain band for the 500 mode ($\hbar\Omega' \approx -6$ eV/Å) and zz -polarized light therefore dominate the RRS spectra. In order to obtain this agreement, the calculated ϵ_2 's had to be broadened by 0.12 eV as mentioned above; otherwise the calculated 500-mode zz spectrum would have consisted of tall, sharp peaks at $2.50, 2.90,$ and 3.15 eV.

The agreement between theory and experiment is of similar quality for the 6 times weaker 435 mode in zz polarization. In the calculation nearly all the intensity (solid line) is due to mixing with the O(4) vibration, as suggested by Rashba and Sherman.⁸ We used the eigenvector component $e(435, O(4)) = 0.47$. The pure O(3)+O(2) mode (dashed line) does not move the chain band, and the amount by which it moves the top of the O(2)(z)-Cu(2)($3z^2-1$)-O(4)(z) band is negligible. For the 340 mode the calculated intensity in zz polarization is 40 times weaker than for the 500 mode, and, here

again, it is mainly due to mixing with the O(4) mode [$e(340, O(4)) = -0.14$]. This mixing, however, seems to be too large because no intensity was detected in the experiment. By neglecting the O(4) mixing, but keeping the strong mixing between O(3)+O(2) and O(3)-O(2), which tends to make the 435 mode O(3)-like [O(3) is above the chain oxygen O(1)] and the 340 mode O(2)-like,⁶ the intensity remains close to what was calculated for the pure O(3)-O(2) mode (dashed line).

The 150 and 115 modes were predicted to mix negligibly with the O(4) mode, but to be strong mixtures of the Cu(2) and Ba modes.^{6,7} However, the experimental and theoretical RRS spectra agree only if the pure modes are used for the calculation. That the 150 mode is mainly Cu(2)-like was previously inferred by isotopic substitution of Cu:¹⁷ The 150 mode shows the full isotopic shift while that at 115 does not shift. The strong mixing given by the LDA results from a fortuitous near degeneracy of the pure mode frequencies. The calculated intensity for the pure Cu(2) mode is 25 times weaker than for the 500 mode and is mainly caused by modulation of the Cu(2)-O(2) and Cu(2)-O(4) hopping integrals ($\hbar\Omega' \approx 1.5$ eV/Å). The RRS intensity calculated for the Ba vibration is mainly due to the dipole shift it induced in the chain with respect to the planes. Essentially the same transitions are involved as those responsible for the intensity of the O(4) mode ($\hbar\Omega' \approx 1.5$ eV/Å).

We now interpret the calculated results for xx and yy polarizations. $\epsilon_{2yy}(\omega)$ in Fig. 2 has a large peak at 0.9 eV which is not present in $\epsilon_{2xx}(\omega)$. This peak is caused by transitions between plane and chain bands near the U point where these bands cross, hybridize strongly, and have saddle points or minima. Since the O(4) and the Ba modes shift the chain bands relative to the plane bands, and since the plane-oxygen and the Cu(2) modes deform the plane bands, especially near their saddle points, the Raman profiles for all A_g modes in yy polarization are predicted to have large peaks at 0.9 eV (Fig. 2). Experimental verification of this nontrivial feature of the LDA band structure would be important.

For higher energies the interband transitions for xx and yy polarizations are contributed by several bands with rather small optical matrix elements. Plane-plane transitions have approximate tetragonal symmetry and the ϵ_2 contributions have the characteristic shape of a low-energy onset, which arises from transitions to the Fermi surface, followed by a gradual fall off. Four such contributions, with onsets at $1.0, 1.4, 2.3,$ and 2.6 eV, are present for ϵ_{2xx} ; they also exist for ϵ_{2yy} but are masked by transitions to the chain band. The four initial-state plane bands are, respectively, the two antibonding O(2)(y)-Cu(2)(xy)-O(3)(x) $pd\pi$ bands and the two antibonding O(2)(y)-O(3)(x) bands which bond to, respectively, $Y(z)$ and $Y(x^2-y^2)$. The dispersion of the latter, caused by O-O hopping, is similar to that of the plane bands. Its signature is seen in Fig. 2. Transitions

to the chain band cause xx - yy anisotropy: The feature in ϵ_{2yy} around 2.4 eV is mostly due to chain-chain transitions from the O(4)(y)-O(1)(z) band. Another contribution to ϵ_{2yy} is from the two antibonding Cu(2)(yz)-O(3)(z) $pd\pi$ plane bands which are parallel to the chain band, but split by the interplane interaction via the O(3)(z) orbitals. The corresponding structure starts with transitions to the Fermi surface at 2.6 eV, steps up at 2.8 eV (from the Y to the T point, interplane antibonding), down at 3.3 eV (S - R), and terminates above 4 eV (Y - T , interplane bonding). The matrix element is $\langle yz|y|z \rangle$ on Cu(2). The analogous Cu(2)(xz)-O(2)(z) $pd\pi$ plane bands disperse in the k_x rather than in the k_y direction so that the contribution to ϵ_{2xx} extends all the way from 1.0 to 4.5 eV. It steps up at 1.8 eV (interplane bonding to the Fermi surface) and 2.8 eV (S point), and down at 3.3 eV (R).

The Raman intensity for the O(4) mode and yy polarization is calculated to be 50 times less than for zz , but several times larger than for xx . It peaks at 2.4, 2.9, and 3.3 eV, and is mainly caused by the above-mentioned transitions to the chain band from the O(4)(y)-O(1)(z) and Cu(2)(yz)-O(3)(z) bands. The agreement with the experimental spectrum and x - y anisotropy is good. For the pure Ba mode the calculated RRS spectrum and anisotropy is similar because moving Ba away from the chain causes the potential at Cu(1) and O(1) to increase with respect to that in the planes.

For the pure Cu(2) mode the calculated intensity is weak in both polarizations. There are peaks at the above-mentioned onsets of plane-plane transitions as well as those due to the $pd\pi$ plane-chain transitions. For xx polarization, the 2.6-eV plane-plane and the 2.8-eV Cu(2)(xz)-O(2)(z) plane-chain transitions reinforce each other. The intensity calculated for the pure O(3)+O(2) mode is larger due to the smaller mass, but the underlying mechanisms are similar. One important exception is that now also the interplane interactions via the plane oxygens, and possibly Y , are modulated. The enforcement of the 2.6- and 2.8-eV xx transitions is stronger. Moreover, the deformation potential for the plane-plane transitions now adds constructively to that of the Cu(2)(xz)-O(2)(z) plane-chain transitions. The mixing of the 435 mode is essential to reduce its RRS intensity, in agreement with the experiment. The Raman spectra are dominated by the plane-plane plus Cu(2)(yz)-O(3)(z) plane-chain transitions for the 435 mode [mainly O(3)], and by the plane-plane plus Cu(2)(xz)-O(2)(z) plane-chain transitions for the 340 mode [mainly O(2)]. The intensity of the pure plane-oxygen modes would vanish without any dimpling, as is indeed observed for the Tl- (or to a lesser extent for Bi)-based superconductors.

We have presented the first resonant Raman spectra for the five A_g phonon modes of $\text{YBa}_2\text{Cu}_3\text{O}_7$ as well as first-principles LDA calculations of the Raman efficiencies. Good agreement between theory and experi-

ment allows a detailed interpretation in terms of LDA band shifts and specific interband transitions. In particular, the position and deformation potentials of the chain band which crucially influences the zz -polarized spectra are correctly described by our calculations. Concerning the plane bands, only the region near the Fermi surface is relevant for the dielectric function or the RRS. Thus, we are not able to verify the position of the top of the plane bands. From the RRS, one also obtains information about the mode mixing: Ba and Cu phonons seem to be essentially pure while the three oxygen modes mix strongly in such a way that the 340 mode has little O(4) content.

We thank J. Kircher for supplying us with data of the dielectric properties prior to publication and C. Thomsen for valuable discussions. We acknowledge technical help by H. Hirt, M. Siemers, and P. Wurster. This work was supported by the Bundesminister für Forschung und Technologie, and the European Community. I.I.M. acknowledges support by the A. v. Humboldt Foundation.

^(a)Permanent address: P. N. Lebedev Physical Institute, Leninski pr. 53, Moscow 117924, USSR.

¹For a review, see C. Thomsen and M. Cardona, in *Physical Properties of High Temperature Superconductors*, edited by D. M. Ginsberg (World Scientific, Singapore, 1989), p. 409.

²C. Thomsen, M. Cardona, B. Friedl, C. O. Rodriguez, I. I. Mazin, and O. K. Andersen, *Solid State Commun.* **75**, 219 (1990).

³E. T. Heyen, R. Liu, M. Garriga, B. Gegenheimer, C. Thomsen, and M. Cardona, *Phys. Rev. B* **41**, 830 (1990).

⁴V. B. Timofeev, A. A. Maksimov, O. V. Misochko, and I. I. Tartakovskii, *Physica (Amsterdam)* **162-164C**, 1409 (1989).

⁵R. Liu, C. Thomsen, W. Kress, M. Cardona, F. W. de Wette, J. Prade, A. D. Kulkarni, and U. Schröder, *Phys. Rev. B* **37**, 7971 (1988).

⁶C. O. Rodriguez, A. I. Lichtenstein, I. I. Mazin, O. Jepsen, O. K. Andersen, and M. Methfessel, *Phys. Rev. B* **42**, 2692 (1990).

⁷R. E. Cohen, H. Krakauer, and W. E. Pickett, *Phys. Rev. Lett.* **64**, 2575 (1990).

⁸E. I. Rashba and E. Sherman, *Pis'ma Zh. Eksp. Teor. Fiz.* **47**, 404 (1988) [*JETP Lett.* **47**, 482 (1988)].

⁹J. Kircher, M. K. Kelly, S. N. Rashkeev, M. Alouani, D. Fuchs, and M. Cardona (to be published).

¹⁰J. M. Calleja, H. Vogt, and M. Cardona, *Philos. Mag. A* **45**, 239 (1982).

¹¹E. G. Maksimov, S. N. Rashkeev, S. Yu. Savrasov, and Yu. A. Uspenskii, *Phys. Rev. Lett.* **63**, 1880 (1989).

¹²J. Zaanen, M. Alouani, and O. Jepsen, *Phys. Rev. B* **40**, 837 (1989).

¹³J. Kircher, M. Alouani, M. Garriga, P. Murugaraj, J. Maier, C. Thomsen, M. Cardona, O. K. Andersen, and O. Jepsen, *Phys. Rev. B* **40**, 7368 (1989).

¹⁴O. K. Andersen, *Phys. Rev. B* **12**, 3060 (1975).

¹⁵C. Thomsen, M. Cardona, B. Gegenheimer, R. Liu, and A. Simon, *Phys. Rev. B* **37**, 9860 (1988).

¹⁶W. Pickett, *Rev. Mod. Phys.* **61**, 433 (1989).

¹⁷A. Mascarenhas, H. Katayama-Yoshida, J. Pankove, and S. K. Deb, *Phys. Rev. B* **39**, 4699 (1989).